Int J Mater Form (2015) 8:379–389
DOI 10.1007/s12289-014-1179-6

ORIGINAL RESEARCH

Pultrusion of a vertical axis wind turbine blade part-I: 3D thermo-chemical process simulation

Ismet Baran · Cem C. Tutum · Jesper H. Hattel · Remko Akkerman

Received: 25 December 2013 / Accepted: 11 May 2014 / Published online: 29 May 2014

Abstract A novel three dimensional thermo-chemical simulation of the pultrusion process is presented. A simulation is performed for the pultrusion of a NACA0018 blade profile having a curved geometry, as a part of the DeepWind project. The finite element/nodal control volume (FE/NCV) technique is used. First, a pultrusion simulation of a U-shaped composite profile is performed to validate the model and it is found that the obtained cure degree profiles match with those given in the literature. Subsequently, the pultrusion process simulation of the NACA0018 profile is performed. The evolutions of the temperature and cure degree distributions are predicted inside the heating die and in the post-die region where convective cooling prevails. The effects of varying process conditions on the part quality are investigated for two different heater configurations and with three different pulling speeds. Larger through-thickness gradients are obtained for the temperature and degree of cure as the pulling speed increases. This will affect the process induced residual stresses and distortions during manufacturing.

Keywords Pultrusion process · Curing · Finite element analysis · NACA0018 airfoil · Thermosetting resin

I. Baran (✉) · J. H. Hattel
Department of Mechanical Engineering, Technical University of Denmark, 2800 Kongens Lyngby, Denmark
e-mail: isbar@mek.dtu.dk

C. C. Tutum
Department of Electrical and Computer Engineering, Michigan State University, East Lansing, MI, USA

R. Akkerman
Faculty of Engineering Technology, University of Twente, 7500AE Enschede, The Netherlands

Introduction

The EU funded DeepWind Project [1, 2] develops a novel concept for a floating offshore vertical axis wind turbine (VAWT) based on the Darrieus design. The main objective of DeepWind is to develop more cost-effective MW-scale wind turbines through innovative technologies for the sea environment rather than advancing existing concepts (i.e. either a horizontal or a vertical axis wind turbine) that are based on onshore technology. Hence the main challenges of the project are to increase the simplicity of the design and the manufacturing techniques as well as to reduce the total cost of an installed offshore wind farm. The concept is aiming at large-scale wind turbines for deep water. The up-scaling potential of the project is 20 MW wind turbines. It is expected that the structural design can be improved to have a higher strength-to-weight ratio for larger chord lengths, e.g. 10–20 m, with a deep water offshore floating system (100–1000 m).

The blade cross section for the VAWT can be constant along the length of the blade. The pultrusion technology is foreseen to be one of the most efficient and suitable methods to manufacture such a composite blade with a constant profile having a large chord. A VAWT blade has already been manufactured by using the pultrusion process, as reported in [3]. Pultrusion is a continuous, automated closed-moulding process, and it is cost effective for high volume production of products with a constant cross section along the length of the part. Figure 1 presents a schematic view of the pultrusion process. Since it is a continuous process, there is little waste material being produced at the start up and the end of the process. It has been widely used for manufacturing highly strengthened continuous fibre composite structures, e.g. stiffeners in wind turbine blades, reinforcements of concrete elements in the construction industry,

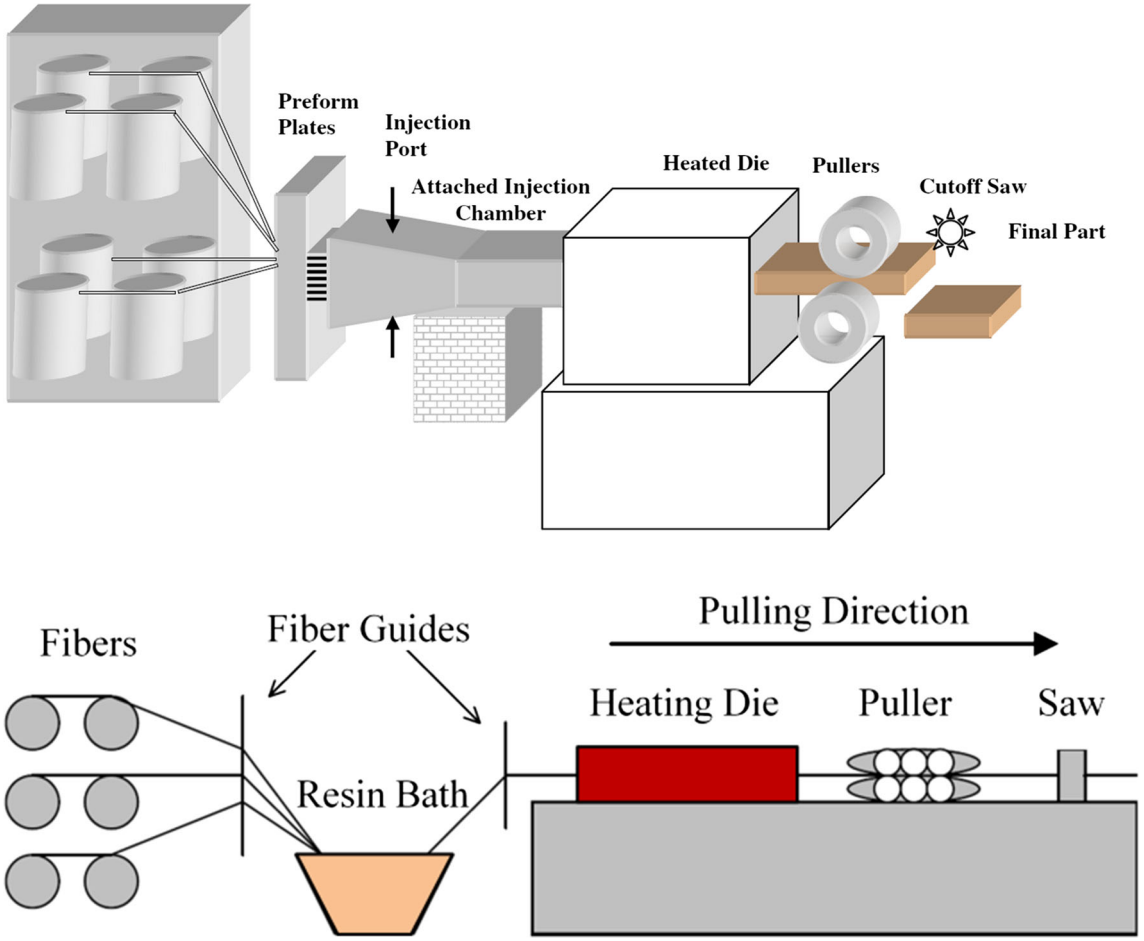

Fig. 1 A schematic view of the pultrusion process with resin injection chamber (*top*) [4] and with open resin bath (*bottom*). Fibers and resin matrix are pulled together in the pultrusion direction by the pullers through the heated die and then the cured composite is cut by a saw system

spars of ship hulls, thin wall panel joiners, door/window frames, drive shafts of vehicles, etc. Producing large blades in one piece using a single die will lead to cost reduction for large series production. The pultruded blades can achieve very high stiffness and resistance against aerodynamic loads as well as vibrations. In principle, a production facility with a relatively short die length, e.g. 1–3 m, can be put on a ship. Manufacturing near to the location of the wind turbine installation which will alleviate transportation issues for these large constructions.

Keeping the multi-physics and large amount of variables involved in the composite manufacturing processes in mind, a satisfactory experimental analysis for the production requires considerable time which is obviously not a cost-efficient approach. Therefore, the development of suitable computational models is highly desired in order to analyze the process for different processing conditions. In literature, there have been several numerical analyses for the pultrusion of relatively simple geometries [4–19]. Generally, thermo-chemical analyses [5, 6, 8, 11], flow simulations [4, 18] and optimizations [7, 10, 13, 19] have been performed using numerical modelling techniques. Material behaviour, transport phenomena, material properties and process models need to be well defined in order to properly simulate the pultrusion process. The description of the material behaviour needs to include the resin kinetics and the chemorheology of the resin system. The transport phenomena involve the heat (and mass due to fluid flow) transfer during the process. A complete description of the pultrusion process requires a thorough understanding of the resin flow, heat transfer, pressure, force (pulling, friction forces etc.) as well as residual stresses and distortions via corresponding numerical models. In the following, some important numerical studies related to the pultrusion are reviewed in detail.

Transient and steady state temperature and cure degree profiles of the composite and the heating die systems during the pultrusion process have been simulated by using numerical techniques such as the finite difference (FD) method and the finite element (FE) method with the control volume (CV) technique or nodal control volume (NCV) technique [4–19]. In [5], the effects of the thermal contact resistance

(TCR) at the die-part interface on the pultrusion process have been investigated by using the CV/FD method and it was found that the use of a variable TCR is more accurate than the use of a uniform TCR for simulation of the process. In [6–8], the simulations of the pultrusion process have been performed using the FE/NCV method. The effects of the resin shrinkage and temperature-dependent material properties on the temperature and the cure degree distributions have been discussed in [12] by using the FE/NCV technique. In [14], the reliability estimation of the pultrusion process of a flat plate was analyzed by using the first order reliability method (FORM). The effect of the uncertainties in the material and resin kinetic properties as well as process parameters on the product quality (i.e. the degree of cure) were investigated [14]. The variations in the activation energy as well as the density of the resin were found to have a strong influence on the degree of cure at the die exit whereas the other process parameters have smaller influences. In [19], the productivity of the pultrusion process for a composite rod was improved by using a mixed integer genetic algorithm (MIGA) such that the total number of heaters was minimized while satisfying the constraints for the maximum composite temperature, the average degree of cure at the die exit and the pulling speed. In addition to the theoretical modelling of the pultrusion process, experimental studies on the pultrusion of various composite profiles such as rods, plates, I-beams etc. have been carried out in [20–26]. Pultrusion of an I-beam was numerically modelled in [22–24] and the predicted temperature and cure degree values were compared with measurements. Die and post-die analyses were performed for a thin uni-directional (UD) carbon/epoxy rod in [26] and the corresponding temperature and cure degree profiles were predicted for different heater configurations, pulling speeds and fiber volume fractions. The effects of convective cooling at the post-die region were also taken into account in the numerical model. The correct prediction of the post die curing (3-4 %) and the temperature distribution is essential for the accurate prediction of the residual stress during the cooling of the composite (after the exit from the die).

So far, the pultrusion process of a relatively thick composite having a curved cross sectional geometry such as the NACA0018 profile has not been described in the referred publications. A numerical simulation tool embracing the pultrusion blade manufacturing process is being developed as part of the DeepWind project. The process parameters affect the efficiency of the process as well as the quality of the product. Usually the process is optimized on a trial-and-error bases. Within the DeepWind project we aim to optimize the process more efficiently using a model based approach. The present paper in particular deals with the thermo-chemical modelling of the pultrusion process for a UD glass/epoxy NACA0018 blade profile. A three-dimensional (3D) thermo-chemical process simulation of a pultruded U-shaped cross section is first performed as a validation of the implemented FE/NCV method, using the data from similar analyses in the literature [7, 8]. Following the validation case, the same modelling strategy has been applied for the pultrusion of the NACA0018 profile in which the post-die region is also included in the model. The model predicts the temperature and the degree of cure distributions at steady state. The effects of the process parameters such as the heater configurations and the pulling speed on the quality of the profile are investigated.

Governing equations

Energy equations

The 3D transient heat transfer equations for the composite part and the die block can be written in a Cartesian coordinate system (Eulerian formulation) as, respectively,

$$\rho_c Cp_c \left(\frac{\partial T}{\partial t} + u \frac{\partial T}{\partial x_1} \right) = k_{x_1,c} \frac{\partial^2 T}{\partial x_1^2} + k_{x_2,c} \frac{\partial^2 T}{\partial x_2^2} + k_{x_3,c} \frac{\partial^2 T}{\partial x_3^2} + q \tag{1}$$

$$\rho_d Cp_d \frac{\partial T}{\partial t} = k_{x_1,d} \frac{\partial^2 T}{\partial x_1^2} + k_{x_2,d} \frac{\partial^2 T}{\partial x_2^2} + k_{x_3,d} \frac{\partial^2 T}{\partial x_3^2} \tag{2}$$

where T is the temperature, t is the time, u is the pulling speed, ρ is the density, Cp is the specific heat, k_{x_1}, k_{x_2} and k_{x_3} are the thermal conductivities in the x_1-, x_2- and x_3-direction, respectively. Here, x_1 is defined as the pulling direction, x_2 and x_3 are the transverse directions. The subscripts c and d correspond to the composite and the die, respectively. Lumped material properties are used and assumed to be constant. The volumetric internal heat generation (q) [W/m^3] due to the exothermic reaction of the epoxy resin is expressed as

$$q = (1 - V_f)\rho_r Q \tag{3}$$

where V_f is the fiber volume fraction, ρ_r is the resin density and Q is the specific heat generation rate [W/kg] due to the exothermic resin cure reaction.

Cure kinetics

The exothermic chemical reaction of the resin is described by the cure kinetics equation. The degree of cure (α) of the resin is equal to the ratio of the amount of heat generated ($H(t)$) during curing, to the total heat of reaction H_{tr} [15]:

$$\alpha = \frac{H(t)}{H_{tr}} \tag{4}$$

The reaction rate, $R_r(\alpha, T)$, can be expressed for an n^{th} order reaction as [15]:

$$R_r(\alpha, T) = \frac{\mathrm{d}\alpha}{\mathrm{d}t} = \frac{1}{H_{tr}} \frac{\mathrm{d}H(t)}{\mathrm{d}t} = K_o \exp\left(-\frac{E}{RT}\right)(1-\alpha)^n \quad (5)$$

where K_o is the pre-exponential constant, E is the activation energy, R is the universal gas constant and n is the order of reaction (kinetic exponent). K_o, E, and n can be obtained by a curve fitting procedure applied to the experimental data evaluated using the differential scanning calorimetry (DSC) [20]. The specific heat generation rate, Q (in Eq. 3), is then calculated as [15]

$$Q = H_{tr} R_r(\alpha, T) \quad (6)$$

The Eulerian formulation used here requires the spatial derivatives rather than the material derivatives as in Eq. 5 ($d\alpha/dt$). The spatial derivatives can be found from relation given in Eq. 7.

$$\frac{\mathrm{d}\alpha}{\mathrm{d}t} = \frac{\partial \alpha}{\partial t} + \frac{\partial \alpha}{\partial x_1}\frac{\mathrm{d}x_1}{\mathrm{d}t} = \frac{\partial \alpha}{\partial t} + u\frac{\partial \alpha}{\partial x_1} \quad (7)$$

and from Eq. 7, the resin kinetics equation can be expressed as

$$\frac{\partial \alpha}{\partial t} = R_r(\alpha, T) - u\frac{\partial \alpha}{\partial x_1} \quad (8)$$

which is used in the transient thermo-chemical model.

Numerical implementation

The FE/NCV approach as described in [15] was implemented in a commercial FE software ABAQUS [27] to model the pultrusion process. The representation of the FE/NCV grid is illustrated in Fig. 2(left). CVs are defined at the nodes of each finite element and the temperature is calculated using the finite element method. The degree of cure, on the other hand, is calculated in the NCVs using the user defined subroutines in ABAQUS. The non-linear internal heat generation (3) together with the cure kinetics (5) are coupled with the energy (1) in an explicit manner in order to obtain a straightforward and fast numerical procedure. The degree of cure is subsequently updated explicitly for each CV using Eq. 8 in its discretized form. This time-stepping procedure is illustrated in the flowchart in Fig. 2(right). In order to obtain stable results and to prevent possible oscillatory behaviour in the numerical implementation, the first order upwind scheme is used for the discretization of the term $(u\partial\alpha/\partial x_1)$ in the cure kinetics equation (see Eq. 9). The criteria for reaching the steady state is defined as the maximum temperature and cure degree increments between the new time step $(n+1)$ and the old time step (n), i.e $\Delta T = max(T^{n+1} - T^n)$ and $\Delta\alpha = max(\alpha^{n+1} - \alpha^n)$, respectively, are set to 0.001 °C and 0.0001, respectively (Fig. 2(right)).

$$\left[\frac{\partial \alpha}{\partial t}\right]^{n \to n+1} = \left[R_r(\alpha, T) - u\frac{\alpha_i - \alpha_{i-1}}{\Delta x_1}\right]^n \quad (9)$$

where the subscript i indicates the particular CV (see Fig. 2(left)), Δx_1 is the distance between the two consecutive CV in the pulling direction and n denotes the time increment.

Validation case

Model description

A 3D thermo-chemical simulation of the pultrusion process for a composite U-shaped profile was performed as a validation case. A UD glass/epoxy was used for the composite material and chrome steel was selected as the die material. The material properties and the cure kinetics parameters are given in Tables 1 and 2, respectively. The material properties of the composite are calculated by a rule of mixtures based on a fiber volume fraction of $V_f = 63.9\ \%$.

The model geometry, shown in Fig. 3, is taken from similar set-ups used in the literature [7, 8]. Only half of the cross section has been considered due to the symmetry, applying an adiabatic thermal boundary condition (BC) at the symmetry surface. Three heating platens are assumed to be

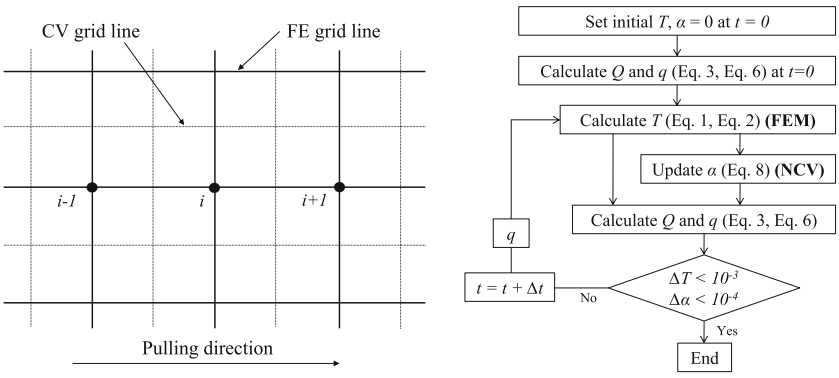

Fig. 2 Schematic view of the FE/NCV grids in the pulling direction (*left*). Flowchart of the time-stepping procedure to solve the equation system for the temperature and the degree of cure (*right*)

Table 1 Thermal properties used in the process simulation [7, 8]

	ρ [kg/m^3]	Cp [J/kg K)	k_{x_1} [W/m K]	k_{x_2}, k_{x_3} [W/m K]
Composite $V_f = 0.639$	2090.7	797.27	0.9053	0.5592
Steel die	7833	460	40	40

placed on the top surface of the die block and the remaining platens are placed on the bottom surface of the die. The corresponding set temperatures of the heaters are given in Table 3. All the surfaces of the die except those on which the heating platens are located are exposed to ambient temperature (27 °C) with a convective heat transfer coefficient of 10 W/(m^2 K). Water-cooled channels are located along the first 90 mm of the die, so that to avoid any premature resin gelation at the inlet of the die. The cross sectional details of the die and the composite including the FE mesh are illustrated in Fig. 4. The element length in the pulling direction is 15 mm. The degree of cure of the composite is equal to zero at the die inlet and the inlet temperature of the composite is taken as the resin bath temperature (45 °C). As in

Table 2 Resin cure kinetics parameters [8]

H_{tr}[kJ/kg]	K_o[1/s]	E[kJ/mol]	n
324	192,000	60	1.69

Table 3 The set temperatures of the heaters (°C) used in the validation case

Heater-1	Heater-2	Heater-3	Heater-4	Heater-5	Heater-6
105.5	148.5	200.0	115.5	146.5	200.0

[7, 8], perfect thermal contact is assumed between the die and the composite.

Results and discussions of the validation case

The degree of cure profiles at steady state shown in Fig. 5 are obtained with a pulling speed of 2.3 mm/s by using the FE/NCV approach inspired by [7, 8]. It is seen that the results match with those in [7, 8]. This shows that the implemented numerical scheme is stable and converged to the correct solution. It is seen from Fig. 5 that point B (along the pulling direction) starts curing before point A. The contribution of the die temperature to the cure degree is more dominant than the contribution of the internal heat generation at the die-part interface (e.g. point B) since point B is closer to the heaters. The reverse is the case for the inner regions of the composite (e.g. point A). However, approximately from $x_1 = 0.6$ m the curing rate of point A is higher than at point B because the internal heat generation plays a more important role at the inner region of the composite. Therefore, although the curing at point A starts at a later stage, the cure degree of point A becomes almost the same as the cure degree of point B at the die exit which is predicted to be approximately 0.89.

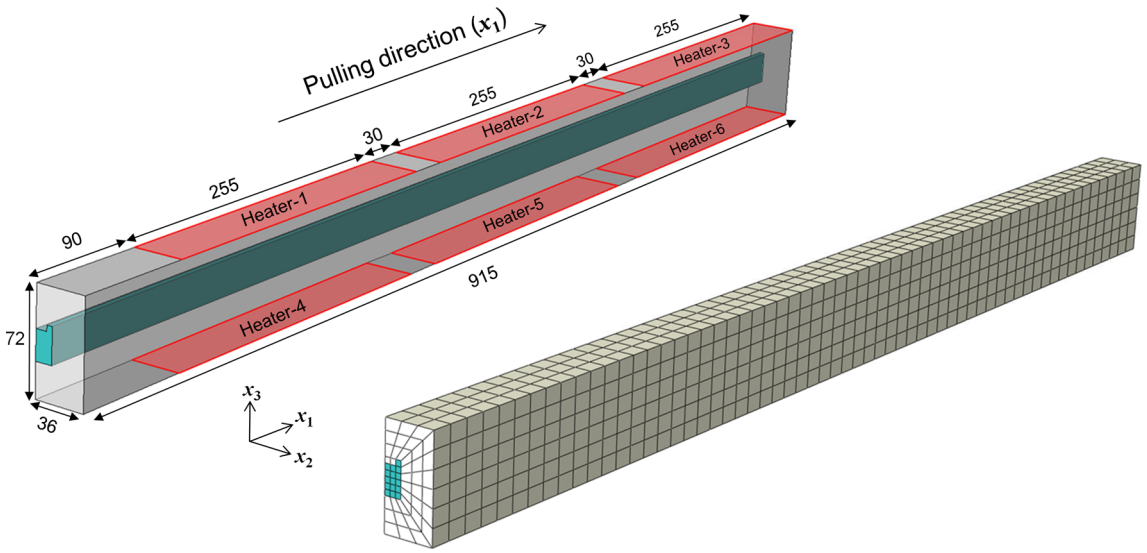

Fig. 3 Symmetric pultrusion model geometry for the U-shaped composite and the corresponding FE mesh in the validation case. All dimensions are in mm

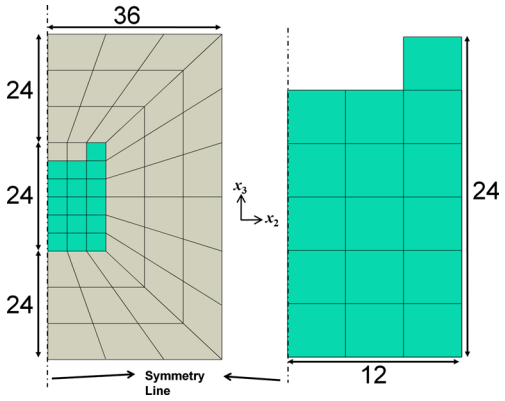

Fig. 4 Cross sectional details of the finite elements for the die (*left*) and the composite (*right*) in the validation case. All dimensions are in mm

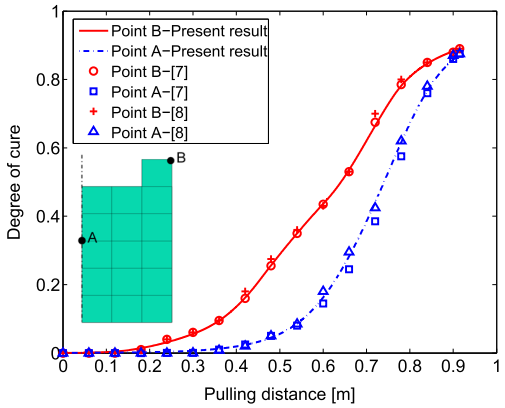

Fig. 5 The predicted degree of cure profiles at points A and B in the validation case

Pultrusion of a NACA0018 profile

Model description

The thermo-chemical analysis implemented in ABAQUS was then used to simulate the pultrusion process of the NACA0018 profile. The schematic representation of the model is seen in Fig. 6. The heater locations are selected similarly to the validation case (in Section "Validation case"); however, in this case only three heating platens on one side are included in the numerical model due to the symmetry. The cross sectional details of the die and the blade including the FE mesh are seen in Fig. 7. The same material properties and BCs are used as in the validation case for the die and the composite. Convective boundaries are defined at the post die region for the exterior surfaces of the blade profile with a convective heat transfer coefficient of 10 W/(m^2 K). The length required to cool the surface of the profile down to room temperature (L_{conv} in Fig. 6) was determined by a trial-and-error analysis, leading to a value for L_{conv} of approximately 9.2 m. Two case studies were carried out based on the set temperature of the heaters which are given in Table 4. The set temperatures of the first case study (Case-1) are assumed to be the same as the first three set temperatures in the validation case. For the second case (Case-2), the corresponding temperatures were taken from [26]. Three different pulling speeds were used for both cases: 2.3 mm/s, 3 mm/s and 5 mm/s, implying total pultrusion process times of approximately 73 min, 56 min and 34 min, respectively, based on the total length of the profile which is approximately 10 m.

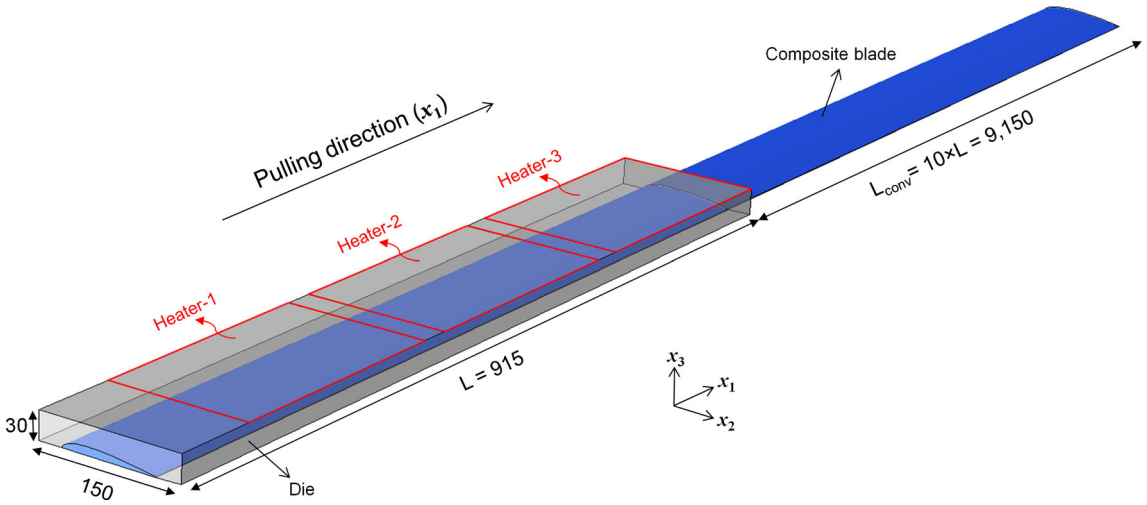

Fig. 6 Schematic of the pultrusion model geometry for the NACA0018 profile including the post die region where convective cooling takes place at the exterior boundaries of the profile. The length of the post die region is not scaled and all dimensions are in mm

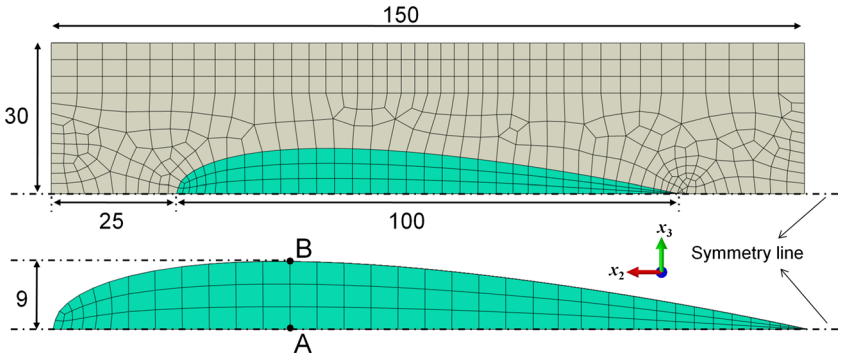

Fig. 7 Cross sectional details of the FE mesh for the die (*top*) and the blade (*bottom*). All dimensions are in mm

Table 4 The set temperatures (°C) of the heaters for the two cases

	Heater-1	Heater-2	Heater-3
Case-1	105.5	148.5	200.0
Case-2	171.0	188.0	188.0

Results and discussion

The predicted temperature and cure degree profiles for Case-1 and Case-2 are presented in Figs. 8 and 9, respectively.

In both cases, the temperature at the die-part interface (e.g. at point B in Figs. 8 and 9) remains almost the same for different pulling speed values due to the prescribed temperature of the heaters. The temperature profile at point A is more sensitive to the increase in pulling speed. The profile shifts to the right for both cases when the pulling speed is increased, illustrating that the convective term ($u\partial T/\partial x_1$) plays a more significant role at the inner regions. The degree of cure distributions follow the same trend: both the temperature and the cure degree profiles at point A shift more to the right than for point B for the two cases as the pulling speed increases. Obviously, also the cure degree profile at point A is more sensitive to the pulling speed than the cure degree profile at point B, higher temperature and final degree of cure values are obtained for this thick-walled section at point A as compared to point B at the end of the process

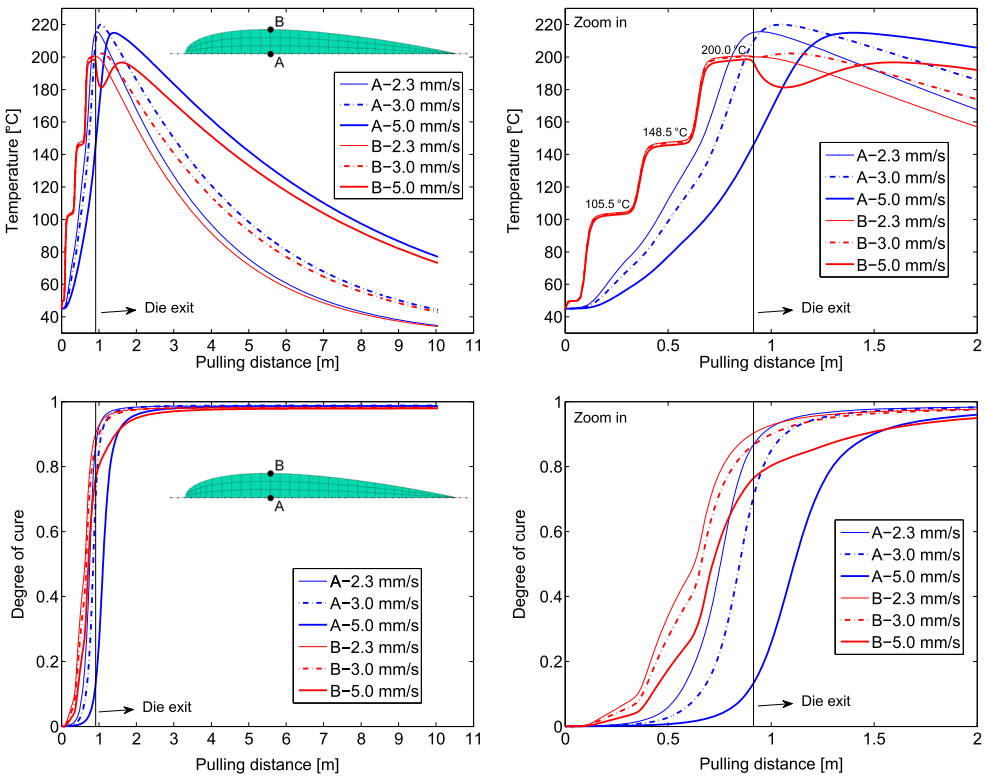

Fig. 8 Temperature (*top*) and cure degree (*bottom*) profiles at points A and B with zoomed plots (*right*) between 0–2 m from the heating die entrance for Case-1 (105.5-148.5-200 °C)

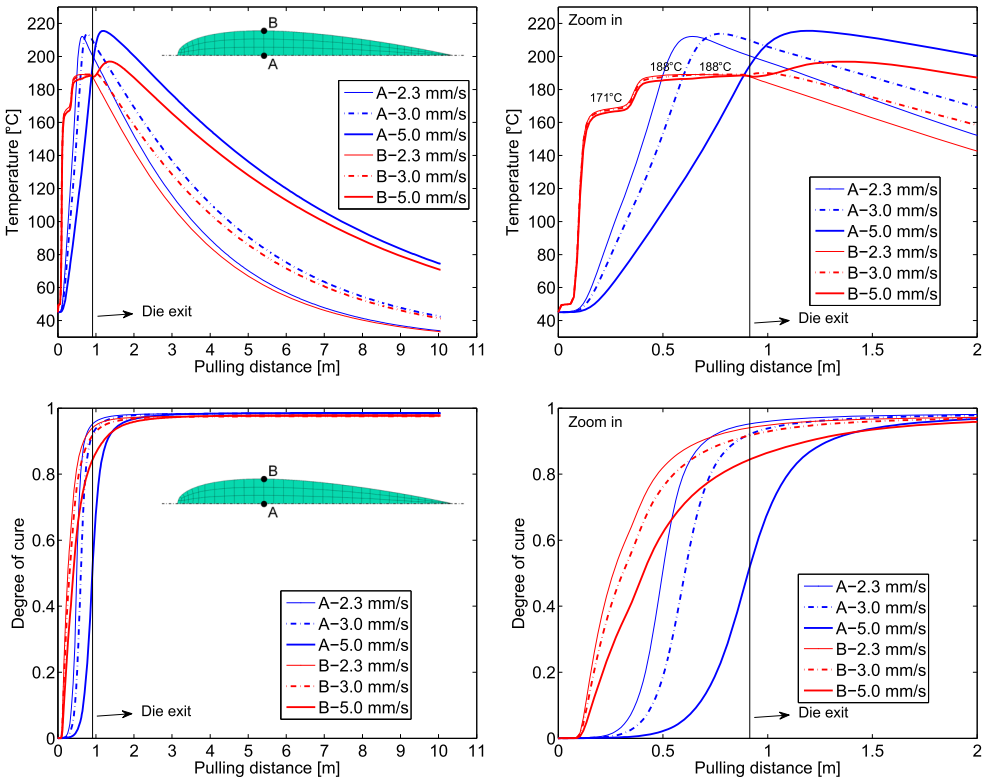

Fig. 9 Temperature (*top*) and cure degree (*bottom*) profiles at points A and B with zoomed plots (*right*) between 0–2 m from the heating die entrance for Case-2 (171-188-188 °C)

as seen from Figs. 8 and 9. In addition, the maximum temperature values at point A are found to be higher than those at point B for all cases. This results in through-thickness temperature and cure degree gradients which together with the heater configuration would have a direct effect on the process induced residual stresses and distortions [28]. The temperature may still increase after the profile has left the die due to exothermic internal heat generation as the curing process continues. In other words, an increase in the pulling speed promotes larger through-thickness gradients of temperature and degree of cure in both cases. The pulling speed has a negative effect on the cure degree at the die exit, i.e. it decreases with an increase in speed; however, this effect vanishes at the end of the process where almost the same cure degree values are obtained for different pulling speeds in both cases (Figs. 8 and 9).

The curing starts earlier in Case-2 due to the higher set temperatures for the first and second heaters (Fig. 9) as compared to Case-1. Therefore, higher cure degree values prevail at the die exit for Case-2. The cure degree values at the die exit and also at the end of the process together with the corresponding % increase in the cure degree are given in Tables 5 and 6 for Case-1 and Case-2, respectively. It is seen that the increase in cure degree, from die exit to the end of the process, becomes larger with an increase in the pulling speed. It should be noted that, even though the cure degree at point A in Case-1 is relatively small at the die exit for a pulling speed of 5 mm/s (i.e. 0.13 in Table 5), surprisingly an increase of more than six times in the cure degree is found (see also Fig. 8(bottom)). This is due to the wall thickness differences leading to an additional variation through the profile cross section (along the chord). Some regions, particularly thinner, cure faster than the region where point A is located (i.e. the thickest region). In addition, high temperature of the regions close to the die surface act as a heater at the post die region

Table 5 The degree of cure values at the die exit ($x_1 = 0.915$ m) and the end of the process ($x_1 \approx 10$ m) for Case-1 (105.5 - 148.5 - 200 °C) with three different pulling speeds

	Point A			Point B		
	Die exit	End of process	Increase (%)	Die exit	End of process	Increase (%)
2.3 mm/s	0.87	0.99	13.5	0.90	0.98	9.1
3 mm/s	0.71	0.99	38.8	0.87	0.98	12.6
5 mm/s	0.13	0.99	658.4	0.77	0.98	27.1

Table 6 The degree of cure values at the die exit ($x_1 = 0.915$ m) and the end of the process ($x_1 \approx 10$ m) for Case-2 (171-188-188 °C) with three different pulling speeds

	Point A			Point B		
	Die exit	End of process	Increase (%)	Die exit	End of process	Increase (%)
2.3 mm/s	0.95	0.99	4.0	0.94	0.98	4.5
3 mm/s	0.92	0.98	6.8	0.91	0.98	7.1
5 mm/s	0.52	0.98	89.4	0.85	0.98	14.7

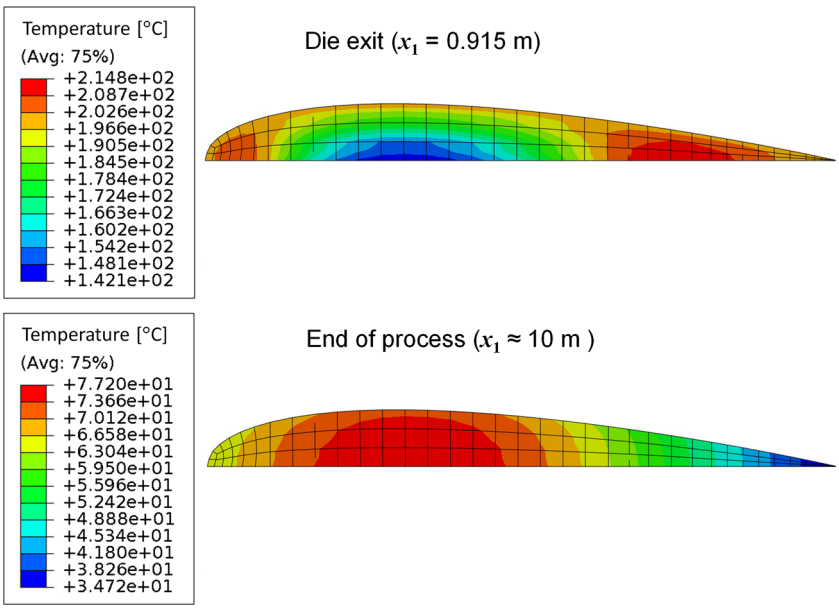

Fig. 10 Temperature distributions inside the blade profile at the die exit (*top*) and at the end of the process (*bottom*) for Case-1 (105.5-148.5-200 °C) with a pulling speed of 5 mm/s

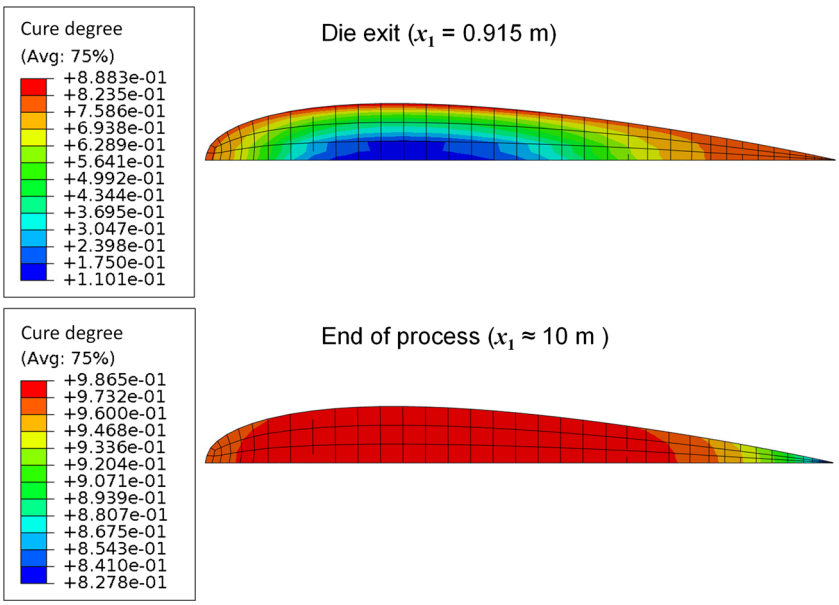

Fig. 11 Cure degree distributions inside the blade profile at the die exit (*top*) and at the end of the process (*bottom*) for Case-1 (105.5-148.5-200 °C) with a pulling speed of 5 mm/s

and hence, invoke the exothermic reaction at inner regions. This can be explained in the contour plots given in Figs. 10 and 11 for the temperature and the cure degree distributions, respectively (Case-1 for 5 mm/s). It is seen in Fig. 10 that the temperature in the thinner regions of the profile are found to be between approximately 208–214 °C at the die exit due the rapid curing whereas the temperature is only 142 °C at point A which shows that high through-thickness thermal gradients prevail at the cross section and the curing takes place at earlier stages at the thinner regions as compared with the point A (Fig. 11). Hence, at the post-die, the heat flow is transmitted from the thinner regions to the point A and at the end of the process the thickest section of the profile is found to be almost fully cured (Fig. 11). The large through-thickness variations in temperature and degree of cure may also lead to poor surface quality as well as unwanted surface defects at the end of the process.

Using the proposed numerical tool, designs of various internal cross-section configurations, e.g. reinforcements, stiffeners, spars, etc., can be analysed including the effects of processing parameters on the expected performance. In this way, the simulation can be used to optimize the process in order to obtain the desired mechanical properties of the product.

Conclusion

A thermo-chemical simulation was performed for the pultrusion process of a composite NACA0018 blade. First, a validation case was carried out in which the cure degree distribution of a pultruded U-shaped composite profile was simulated. The implemented numerical model was found to be stable and accurate as compared with the corresponding results in [7, 8]. Subsequently, the temperature and degree of cure evolutions were simulated for the pultrusion of the NACA0018 profile using two different set temperature schemes of the heaters, i.e. Case-1 (105.5-148.5-200 °C) [7] and Case-2 (171-188-188 °C) [26], for three different pulling speeds (2.3 mm/s, 3 mm/s and 5 mm/s). The main outcomes of this study are summarized as follows:

- It was found that higher final cure degree values prevail in Case-2 due to the higher set temperatures of the first and second heaters which invoke curing at early stages as compared with Case-1. Hence, the heater configurations as well as the set temperatures of the heaters must be determined to obtain the desired product quality which might require a more advanced process optimization study such as the work presented in [19].
- There is significant curing taking place in the post die region. This shows that high temperature of the regions close to the die surface acts as a heater at the post die region and hence, invokes the exothermic reaction at inner regions. In other words, the skin acts as an insulator for the core such that there exists a self accelerating cure reaction.
- Although the degree of cure at the die exit decreases with an increase in the pulling speed, almost the same degree of cure values are obtained at the end of the process for different pulling speeds in both cases due to the continued chemical reaction in the post die region.

This study clearly shows the importance of the process parameters such as the set temperatures of the heaters and the pulling speed on the quality, i.e. curing behaviour, in pultrusion of a composite NACA0018 blade. This directly affects the expected mechanical properties of the product as well as the possibility of the defects and process induced residual stresses. The results provide essential input to the prediction of process induced residual stresses and subsequent simulations of the mechanical performance of the pultruded wind turbine components under appropriate loading conditions and can hence be used to optimise the process, the design and the part performance.

Acknowledgements This work is a part of DeepWind project which has been granted by the European Commission (EC) under the FP7 program platform Future Emerging Technology.

References

1. Schmidt PU, Vita L, Aagaard MH, Hattel JH, Ritchie E, Leban KM, et al. (2012) 1st DeepWind 5 MW baseline design. Energy Procedia 24:27–35
2. Paulsen US, Madsen HA, Hattel JH, Baran I, Nielsen PH (2013) Design optimization of a 5 MW floating offshore vertical-axis wind turbine. Energy Procedia 35:22–32
3. Sutherland HJ, Berg DE, Ashwill TD (2012) A retrospective of VAWT technology. Sandia report, SAND2012-0304
4. Palikhel DR, Roux JA, Jeswani AL (2012) Die-attached versus die-detached resin injection chamber for pultrusion. App Compos Mat. doi:10.1007/s10443-012-9251-1
5. Baran I, Tutum CC, Hattel JH (2013) The effect of thermal contact resistance on the thermosetting pultrusion process. Compos Part B- Eng 45:995–1000
6. Ahmed F, Joshi SC, Lam YC (2004) Three-dimensional FE-NCV modeling of thermoplastic composites pultrusion. J Thermoplast Compos 17:447–462
7. Joshi SC, Lam YC, Win Tun U (2003) Improved cure optimization in pultrusion with pre-heating and die-cooler temperature. Compos Part A-Appl S 34:1151–1159
8. Carlone P, Palazzo GS, Pasquino R. (2006) Pultrusion manufacturing process development by computational modelling and methods. Math Comput Model 44:701–709
9. Baran I, Tutum CC, Hattel JH (2013) The internal stress evaluation of the pultruded blades for a Darrieus wind turbine. Key Eng Mater 554–557:2127–2137
10. Tutum CC, Baran I, Hattel JH (2013) Utilizing multiple objectives for the optimization of the pultrusion process. Key Eng Mater 554–557:2165–2174

11. Joshi SC, Chen X. (2010) Time-variant simulation of multi-material thermal pultrusion. Appl Compos Mater 18:283–296
12. Joshi SC, Lam YC (2001) Three-dimensional finite-element/nodal-control-volume simulation of the pultrusion process with temperature-dependent material properties including resin shrinkage. Compos Sci Technol 61:1539–1547
13. Carlone P, Palazzo GS (2007) Pultrusion manufacturing process development: cure optimization by hybrid computational methods. Comput Math Appl 53:1464–1471
14. Baran I, Tutum CC, Hattel JH (2012) Reliability estimation of the pultrusion process using the first-order reliability method (FORM). App Compos Mat 20:639–653
15. Liu XL, Crouch IG, Lam YC (2000) Simulation of heat transfer and cure in pultrusion with a general-purpose finite element package. Compos Sci Technol 60:857–864
16. Baran I, Tutum CC, Nielsen MW, Hattel JH (2013) Process induced residual stresses and distortions in pultrusion. Compos Part B: Eng 51:148–161
17. Baran I, Hattel JH, Tutum CC (2013) Thermo-chemical modelling strategies for the pultrusion process. App Compos Mat 20(6):1247–1263
18. Carlone P, Baran I, Hattel JH, Palazzo GS (2013) Computational approaches for modeling the multiphysics in pultrusion process. Adv Mech Eng 2013(301875):14. doi:10.1155/2013/301875.
19. Baran I, Tutum CC, Hattel JH (2012) Optimization of the thermosetting pultrusion process by using hybrid and mixed integer genetic algorithms. App Compos Mat 20:449–463
20. Chachad YR, Roux JA, Vaughan JG, Arafat E (1995) Three-dimensional characterization of pultruded fiberglass-epoxy composite materials. J Reinf Plast Comput 14:495–512
21. Liang G, Garg A, Chandrashekhara K (2005) Cure characterization of pultruded soy-based composites. J Reinf Plast Comp 24(14):1509–1520
22. Liu XL (2001) Numerical modeling on pultrusion of composite I beam. Compos Part A-Appl S 32:663–681
23. Liu XL, Hillier W (1999) Heat transfer and cure analysis for the pultrusion of a fiberglass-vinyl ester I beam. Compos Struct 47:581–588
24. Roux JA, Vaughan JG, Shanku R, Arafat ES, Bruce JL, Johnson VR (1998) Comparison of measurements and modeling for pultrusion of a fiberglass/epoxy I-beam. J Reinf Plast Comp 17:1557–1578
25. Sarrionandia M, Mondragn I, Moschiar SM, Reboredo MM, Vzquez A. (2002) Heat transfer for pultrusion of a modified acrylic/glass reinforced composite. Polym Composite 23:21–27
26. Valliappan M, Roux JA, Vaughan JG, Arafat ES (1996) Die and post-die temperature and cure in graphite-epoxy composites. Compos Part B-Eng 27:1–9
27. ABAQUS 6.11 Reference Guide (2011)
28. Bogetti TA, Gillespie JW (1992) Process-induced stress and deformation in thick-section thermoset composite laminates. J Compos Mater 26(5):626–660